

# Multiscale cellulose-based optical management films with tunable transparency and haze fabricated by different bamboo components and mechanical defibrillation approaches

Yu Chen<sup>a,b,1</sup>, Yuting Zhang<sup>a,1</sup>, Juan Long<sup>b,c</sup>, Kaimeng Xu<sup>a,\*</sup>, Tuhua Zhong<sup>b,c,\*\*</sup>

<sup>a</sup> Yunnan Provincial Key Laboratory of Wood Adhesives and Glued Products, International Joint Research Center for Biomass Materials, Southwest Forestry University, Kunming 650224, China

<sup>b</sup> International Centre for Bamboo and Rattan, Beijing 100102, China

<sup>c</sup> Key Laboratory of National Forestry and Grassland Administration, Beijing for Bamboo & Rattan Science and Technology, Beijing 100102, China

## ARTICLE INFO

### Keywords:

Bamboo fibers  
Parenchyma cells  
Micro and nano cellulose  
Optical management film  
Mechanical defibrillation

## ABSTRACT

Renewable cellulose is an outstanding candidate to prepare biomass-based optical management films with tunable transparency and haze. Micro-scale and nano-scale cellulose derived from the parenchyma cells (PC) and bamboo fibers (BF) of *Dendrocalamus sinicus* was first separated and then subjected to succinic esterification and mechanical defibrillation using three different methods: ultrasonication, high-speed blending, and microfluidization. Sustainable multiscale optical management films with tunable haze were obtained by changing the weight ratios of micro/nanoscale cellulose. The PC-based micro/nano cellulose (MNC) films obtained by microfluidization with the highest content of nanoscale cellulose (96.5 %) displayed the highest light transmittance (89.4 %) and tensile strength (164.3 MPa) but the lowest haze (32.0 %) and anti-glare ability. The BF-based MNC films obtained by ultrasonication with the lowest content of nanoscale cellulose (20.4 %) but the highest content of microscale cellulose (79.6 %) showed the highest haze (96.7 %), a medium light transmittance (81.3 %), and the outstanding anti-glare effects. The MNC films with both high in transparency (84.8–87.5 %) and haze (81.5–88.4 %) along with good strength and flexibility can be obtained by tuning the bamboo components and mechanical defibrillation methods. This study provides a green and facile way to fabricate sustainable optical management films.

## 1. Introduction

Optical management films with high transmittance and light diffusivity are widely used in organic light-emitting diode (OLED), solar cells, transistor, touchscreen electrode, optical sensor, and energy-saving buildings (Gao et al., 2019; Hou et al., 2020; Jia et al., 2019; Li et al., 2024; Zhang, Zhang, et al., 2023; Zhao et al., 2023). The optical transparency and haze are two crucial parameters for the excellent candidate of optical management films, which are considered to be mutually exclusive properties (Sun et al., 2021; Zhang, Wang, et al., 2023). Optical management films typically utilize conventional substrates made from nonbiodegradable and nonrenewable petroleum-based polymers and heavy and fragile glass, leading to high energy consumption and significant environmental pollution concerns (Jiang et al., 2023; Sun

et al., 2021).

Highly transparent films with tailorable haze derived from natural resources can be used as optical management materials to enhance light absorption and dispersion uniformity. Renewable, multiscale cellulose including microsized cellulose fibers (MCFs), cellulose nanofibrils (CNFs), cellulose nanocrystals (CNCs), and their mixtures are potential and great candidates to prepare highly transparent and hazy optical management films via various methods, including chemical treatment, vacuum impregnation, dissolve-regeneration, and casting (Hou, Li, et al., 2022; Hu et al., 2021; Li et al., 2024; Shi et al., 2025; Sun et al., 2021; Zhang, Guo, et al., 2022; Zhu et al., 2016). A 2,2,6,6-tetramethylpiperidine-1-oxyl (TEMPO)-oxidized CNFs were deposited by microscale TEMPO-oxidized wood fibers to obtain a highly hazy (62 %) and transparent (88 %) film (Yang et al., 2018). Cellulose paper was

\* Corresponding author.

\*\* Correspondence to: T. Zhong, International Center for Bamboo and Rattan, Beijing 100102, China.

E-mail addresses: [xukm007@163.com](mailto:xukm007@163.com) (K. Xu), [zhongth@icbr.ac.cn](mailto:zhongth@icbr.ac.cn) (T. Zhong).

<sup>1</sup> They contributed equally to this work.

<https://doi.org/10.1016/j.carbpol.2024.122811>

Received 12 June 2024; Received in revised form 24 September 2024; Accepted 25 September 2024

Available online 26 September 2024

0144-8617/© 2024 Elsevier Ltd. All rights are reserved, including those for text and data mining, AI training, and similar technologies.

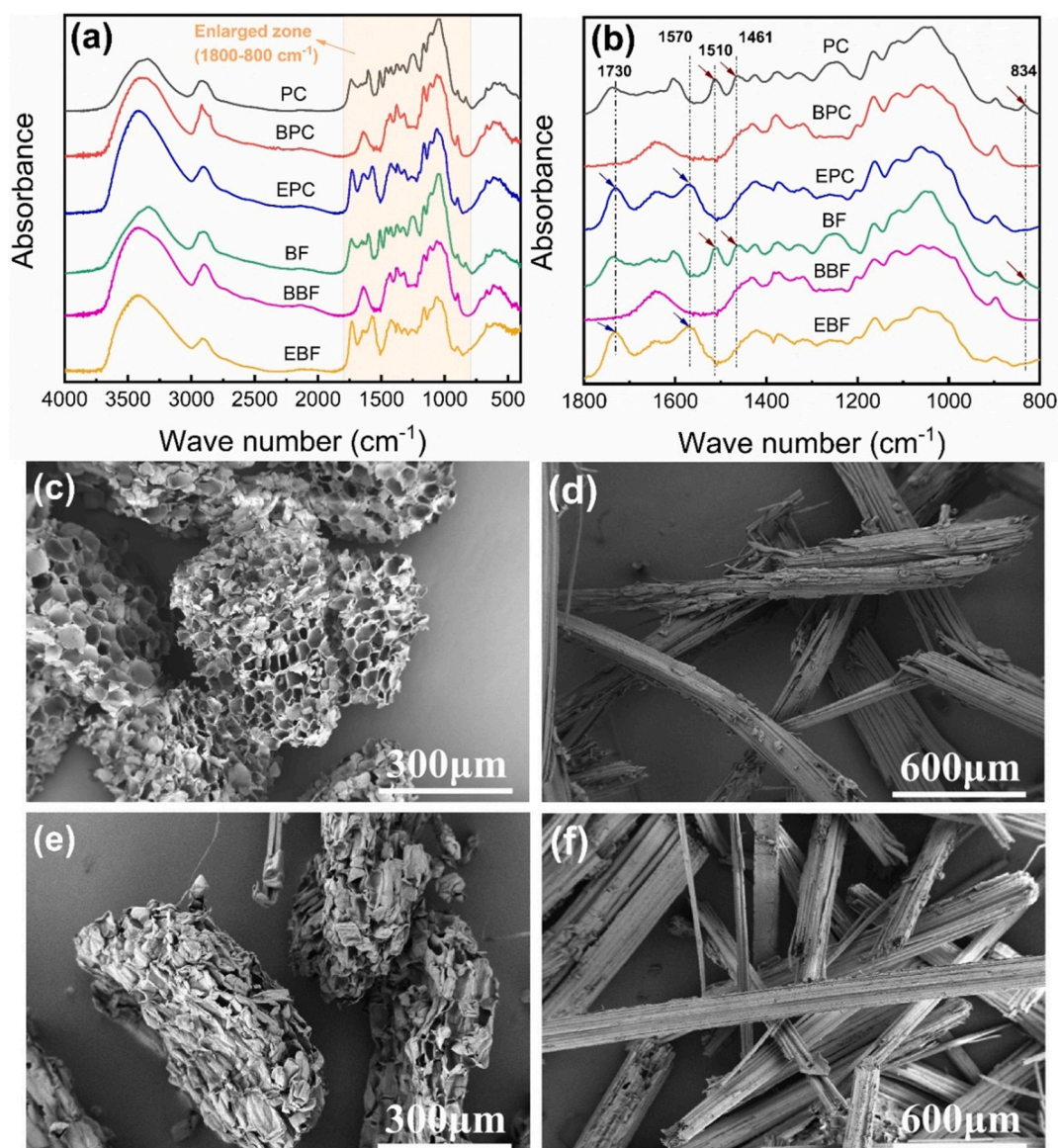


**Fig. 1.** FTIR spectra (a) and its enlarged zone (b) of BF and PC after bleaching and esterification and SEM images of BF and PC before and after bleaching: (c) PC, (d) BF, (e) BPC, and (f) BBF.

**Table 1**

Comparison of the chemical composition, DP, and crystallinity of PC and BF before and after bleaching treatment.

Samples	Cellulose (%)	Hemicellulose (%)	Lignin (%)	DP	Crystallinity (%)
PC	42.9 ± 0.3	17.1 ± 0.5	32.6 ± 0.2	–	46.4
BPC	86.5 ± 0.1	12.9 ± 0.1	0.52 ± 0.05	1251 ± 25	64.4
BF	55.4 ± 0.8	13.0 ± 0.4	29.9 ± 0.4	–	64.4
BBF	89.6 ± 0.5	10.1 ± 0.4	0.33 ± 0.53	1579 ± 13	69.6

chemically modified using trimethylolpropane tris(3-mercaptopropionate) and isophorone diisocyanate by vacuum impregnation to produce an optical management film with light transmission of 84 % and haze of 75 %, respectively (Zhang, Yuan, et al., 2022). A cellulose film with a high transparency (90%) and haze (91 %) was prepared by immersing southern yellow pine microfibril into ionic liquid 1-butyl-3-methylimidazolium chloride (Zhu et al., 2016). An all-cellulose composite film with transmittance of 90.1 % and haze of 95.2 % was fabricated by mixing softwood cellulose fiber and regenerated cellulose by sodium hydroxide/urea solution (Hou et al., 2020). Carboxymethyl cellulose (CMC)/TEMPO-oxidized CNC composite films

obtained by casting showed adjustable optical properties with transparency of 90.87–92.24 % and haze of 3.17–13 % (Li et al., 2024). However, the cellulose solvents and other chemically modifying agents are high cost, long time-consuming, complicated process and the secondary pollution is easily caused after use. Meanwhile, the cellulose solutions with high viscosity are difficult to combine with other functional fillers. This becomes an obstacle for manufacturing all cellulose-based transparent films.

A combination with facile chemical pretreatment and mechanical defibrillation can improve the environmental friendliness, production efficiency of cellulose-based optical management films and reduce their

**Table 2**  
Physical-chemical properties of MNC.

Sample codes	Carboxyl contents (mmol/g)	Crystallinity (%)	Micro-scale cellulose (%)	Nano-scale cellulose (%)
PC-MNC-U	1.85	51.5	71.1	28.9
PC-MNC-B	1.80	44.4	14.2	85.8
PC-MNC-M	1.89	42.7	3.5	96.5
BF-MNC-U	1.76	53.3	79.6	20.4
BF-MNC-B	1.69	50.0	20.0	80.0
BF-MNC-M	1.75	42.5	6.1	93.9

energy consumption during production. A strong and flexible cellulose-based film with both high in transparency (82.7 %) and haze (92.4 %) was produced by combining TEMPO-oxidation pretreatment with ultrasonic homogenization and high-speed blending (Guan et al., 2022). A highly transparent phosphorylated cellulose (PhC) films with above 80 % transparency were obtained from a PhC fiber/water slurry and exhibited a haze of 9–91 % under different mechanical disintegration time by high-speed blending (Hou, Zhao, et al., 2022). Bamboo is one of the fastest growing timber biomasses with abundant availability, outstanding physical, chemical, and mechanical properties as well as excellent biodegradability (Zhao et al., 2024). Cellulose in bamboo mainly derived from two parts: parenchyma cells (PC) and bamboo fibers (BF) (Abe & Yano, 2010; Zhang, Yuan, et al., 2022). Our previous study proposed a facile and green one-pot way by combining rapid succinylation with high-speed blending to fabricate the multiscale cellulose film in the haze range of 59.2 % to 92.3 % with the high transparency (90.5 %) (Chen et al., 2024). However, the degree of fibrillation and its effects on the physical, chemical, mechanical, and optical properties are different when PC and BF are subjected to the same

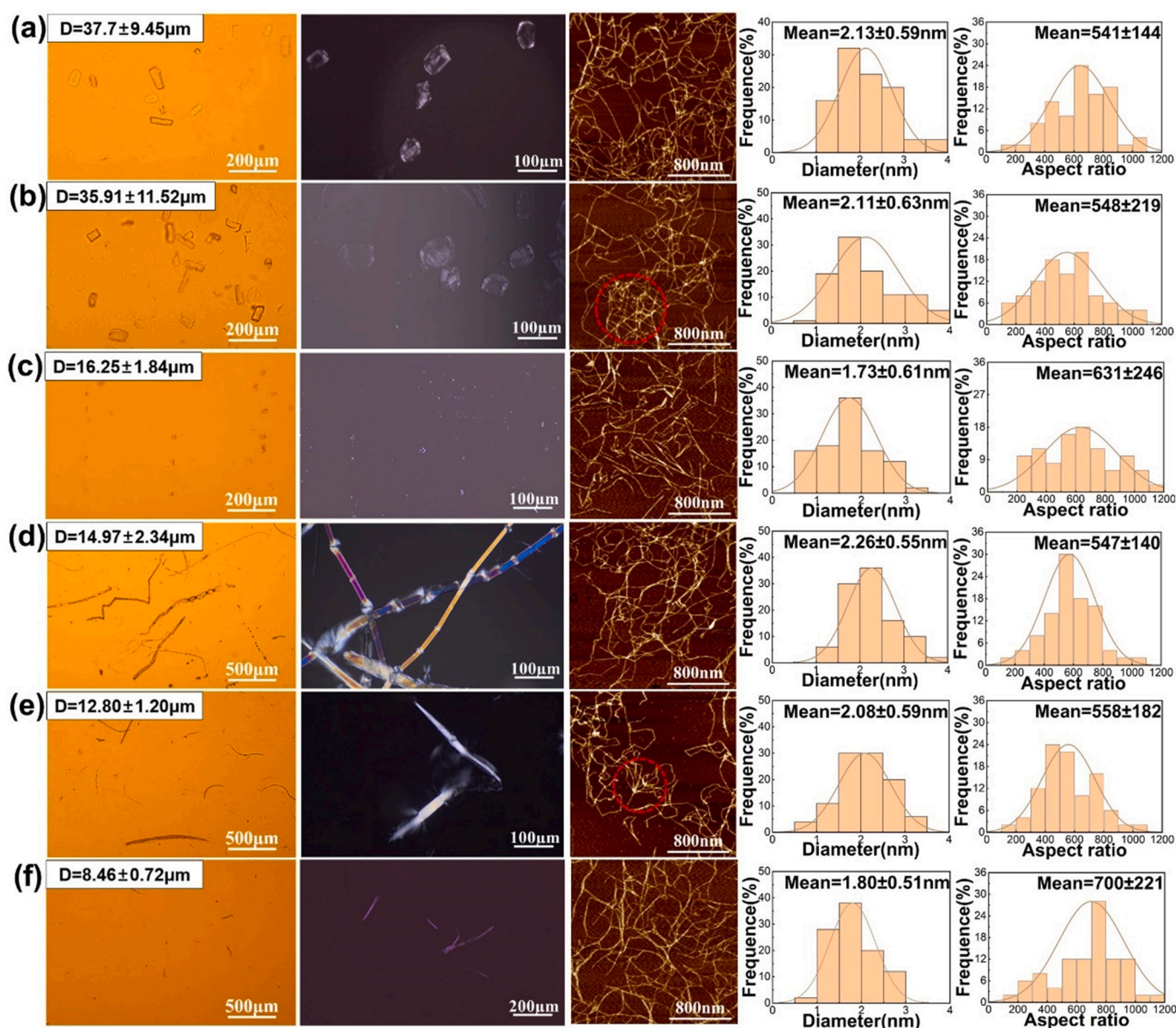


**Fig. 2.** Optical and polarized optical micrographs of micro-scale cellulose and AFM images of nano-scale cellulose and their distributions of width and aspect ratio: (a) PC-MNC-U, (b) PC-MNC-B, (c) PC-MNC-M, (d) BF-MNC-U, (e) BF-MNC-B, and (f) BF-MNC-M.

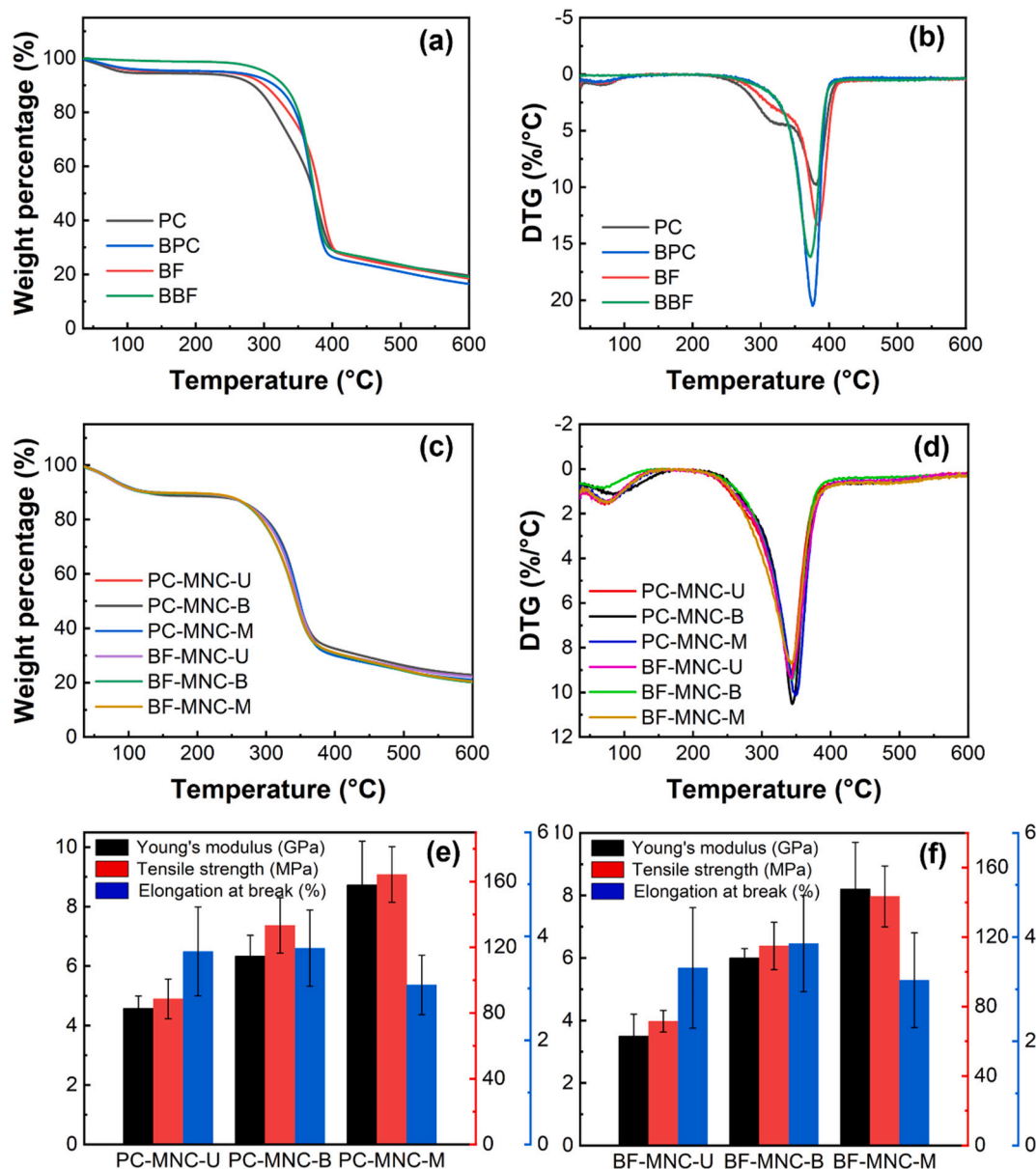


Fig. 3. (a) Typical TG curves and (b) DTG curves of PC and BF before and after bleaching, (c) TG and (d) DTG curves and mechanical properties of the resulting PC-MNC (e) and BF-MNC (f).

chemical modification and mechanical disintegration (Qu et al., 2021; Zhang et al., 2020; Zhou et al., 2022).

In this study, we fabricated multiple scale cellulose films from *Dendrocalamus sinicus*, the largest bamboo in the world. The micro-scale and nano-scale cellulose (MNC) films derived from PC and BF of bamboo were separated and then subjected to succinic esterification and mechanical defibrillation using three different methods: ultrasonication, high-speed blending, and microfluidization. We hypothesized that the cellulose based sustainable and flexible multiscale MNC films with tunable optical properties (transparency and haze) by changing the weight ratios of micro-scale and nano-scale cellulose can be potentially applied for optical management fields including OLED, touchscreen electrode, optical sensor, and energy-saving buildings. The effects of two types of cellulose sources in bamboo and three different mechanical defibrillations on the contents as well as physical and chemical properties of MNC were investigated. The crystallinity, thermal stability, optical and mechanical properties of the resulting optical management films were comprehensively characterized.

## 2. Materials and methods

### 2.1. Materials

*Dendrocalamus sinicus* was obtained from Cangyuan Country, Yunnan Province. Peracetic acid (15–18 %), Potassium hydroxide (KOH), succinic anhydride (SA) and dimethyl sulfoxide (DMSO) with the analytical grades were purchased from Aladdin, China.

### 2.2. Extraction and fractionalization of micro/nano cellulose (MNC)

Bamboo slivers were ground by a shredder (YB-1000A, SuFeng, China) and then immersed in water for 2 min, PC particles were floated onto the water while BF particles were sunk immediately at the bottom because of their difference in density. Subsequently, PC and BF were chemically pre-treated in peracetic acid solution of 8 % at 85 °C for 6 h, respectively to remove lignin. 5 % KOH was used to remove hemicellulose on delignified PC and BF at 90 °C for 2 h. Finally, Bleached PC and

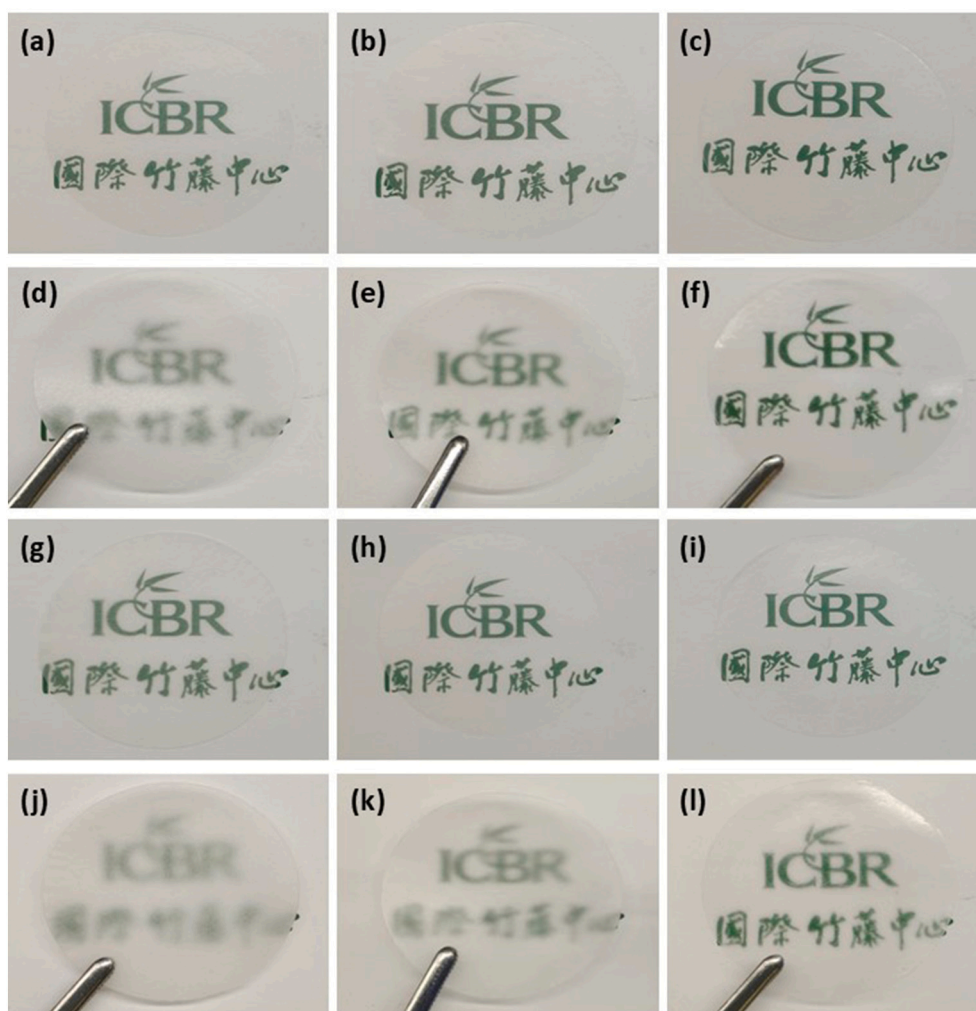


**Fig. 4.** Digital photographs of MNC films closely attached to a baseboard with a logo and lifted 0.5 cm above the baseboard. (a, d) PC-MNC-U; (b, e) PC-MNC-B; (c, f) PC-MNC-M; (g, j) BF-MNC-U; (h, k) BF-MNC-B; (i, l) BF-MNC-M.

BF were obtained and coded as BPC and BBF, respectively. Then, the activation of BPC and BBF (40% solid contents and 2 g dry weight) was carried out in a mixture of DMSO/KOH/H<sub>2</sub>O (88 g/0.8 g/4–6 g) and they were further subject to an esterification reaction with SA at pH = 9.0 corresponding to their codes of EPC and EBF, respectively. Subsequently, the EPC and EBF were mechanical defibrillation using three methods. The ultrasonication was carried out using an ultra-sonicator (JY99-IIDN, Scientz, China) at 540W for 10min with a frequency of 30kHz, a pulse on of 5 s. The resultant samples were labeled as PC-MNC-U and BF-MNC-U, respectively. The high-speed blending was performed at 30000 rpm for 10min with 30s interval rest time every 2 min in a simple kitchen blender (PB210B, Midea, China). The modified samples were labeled as PC-MNC-B and BF-MNC-B, respectively. The microfluidization was performed with a high-pressure microfluidizer (M-110EH-30, Microfluidics, USA) with four passing times in interaction chambers at a pressure of 1500 bar. The obtained samples were labeled as PC-MNC-M and BF-MNC-M, respectively. The micro and nano cellulose was fractionalized using a high-speed centrifuging (Centrifuge 5417C, Eppendorf, Germany) for 10 min at the rotational speed of 12,000 rpm. The clear portion on the top of centrifuge tube was the nano-scale cellulose. The remaining part was the micro-scale cellulose. Then they were dried and calculated their weight ratios.

### 2.3. The fabrication of multiscale MNC films

The MNCs were suspended in deionized water with a concentration of 0.3 wt%, followed by bubble removal in an ultrasonic (KQ5200DE, Kunshan Ultrasonic Instrument, China). Subsequently, the suspensions were cast and then dried at 40 °C for 48 h. The resultant films were placed in a chamber at a relative humidity of 95 % for 1 h and then compressed at 6.125 kPa for 24 h at room temperature for further characterization.

### 2.4. Characterization of micro and nano cellulose

The chemical compositions and the average degree of polymerization (DP) of PC and BF samples before and after bleaching were determined according to the NREL/TP-510-42,618 (Sluiter et al., 2008), and ASTM D1795–13, respectively. The crystallinity index (CrI) of samples were measured with an X-ray diffractometer (D8 Advance A25X, Bruker, Germany) (Segal et al., 1959). The chemical functional groups of PC and BF before and after bleaching and the resultant MNC were characterized using an FTIR spectrometer (Nexus 670, ThermoFisher Scientific, USA). The thermal stability of MNC samples was examined by a thermogravimetric analyzer (TGA4000, PerkinElmer, USA) ranging from 30 °C to 600 °C with a 10 °C/min heating rate. The micro-morphologies of the micro- and nano-scale cellulose separated from the MNC mixture were observed by an optical microscopy (DM LB2, Leica, Germany), a

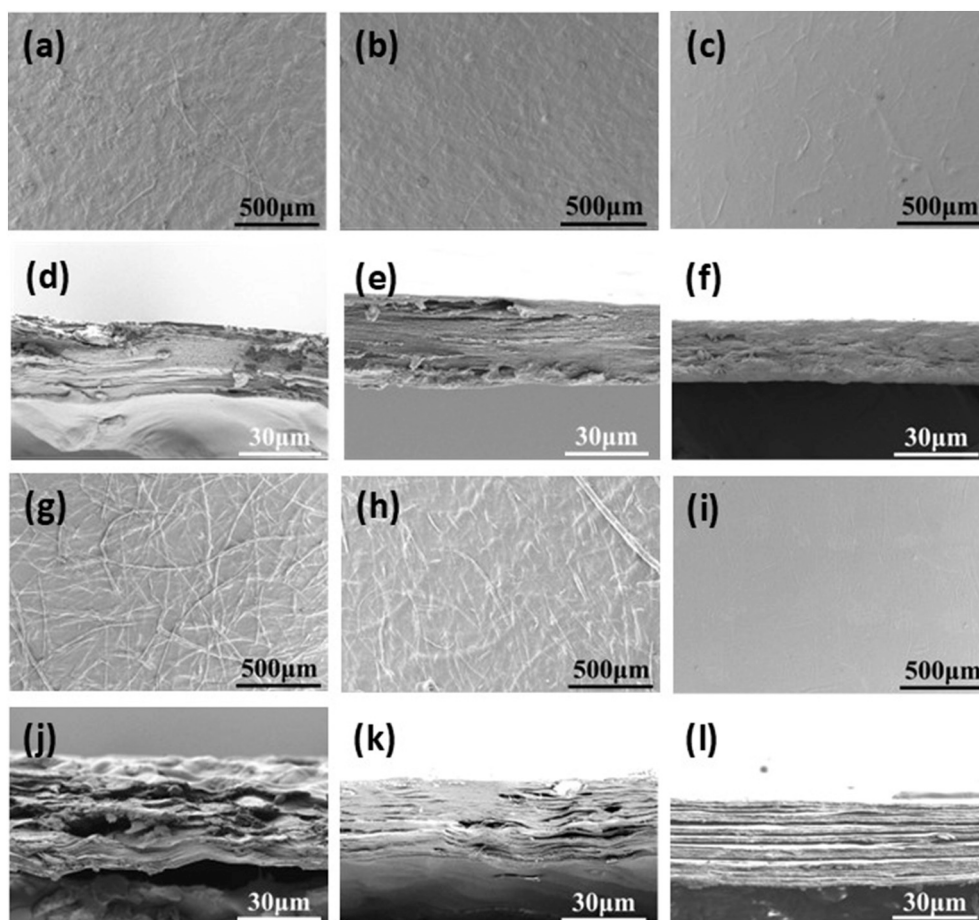


Fig. 5. SEM images of the microstructure of the film surface and fractured surface. (a, d) PC-MNC-U; (b, e) PC-MNC-B; (c, f) PC-MNC-M; (g, j) BF-MNC-U; (h, k) BF-MNC-B; (i, l) BF-MNC-M.

polarized optical microscope (BX53M, Olympus, Japan) equipped with an Olympus DP27 digital camera, and an atomic force microscopy (Icon, Bruker, USA). The variation on carboxylate contents of various MNC samples was tested by conductivity titration method (Zhong et al., 2020).

### 2.5. Evaluation on optical management properties of MNC films

The micro-morphologies of the MNC films were observed by a scanning electron microscopy (Gemini 360, Zeiss, Germany). The hazes of MNC films were assessed by a Haze instrument (TH-110, Hangzhou CHNSpec Technology, China). The angular distribution of transmitted light was evaluated using an angle meter equipped with a xenon lamp (HL-2000, IdeaOptics, China) connected to an optical fiber referring to our previous method (Chen et al., 2024). The tensile test was performed on an electronic mechanical instrument (Instron 5848, Instron, USA) with a load cell of 500 N, an initial clamping separation length of 21.0 mm, and a speed of 0.5 mm/min.

## 3. Results and discussion

### 3.1. Variations in chemical composition, crystallinity, and micro-morphology of PC and BF

FTIR spectra and micro-morphologies of PC and BF before and after bleaching are shown in Fig. 1. The broad peaks in the range of 3650 to 3050  $\text{cm}^{-1}$  for all the samples are associated with the  $-\text{OH}$  stretching vibrations, as seen in Fig. 1(a and b) (Khawas & Deka, 2016). The peak at 1738  $\text{cm}^{-1}$  is related to uronic ester groups in hemicellulose, and the

peaks at 1510  $\text{cm}^{-1}$ , 1461  $\text{cm}^{-1}$ , and 834  $\text{cm}^{-1}$  correspond to aromatic rings in lignin and guaiacyl lignin structures. The characteristic peaks for hemicellulose and lignin significantly became weak and even vanished for both BPC and BBF, which implied that the partial hemicellulose and almost all lignin components had been removed (Fatah et al., 2014; Szcześniak et al., 2008). The two new peaks emerged at 1730  $\text{cm}^{-1}$  and 1575  $\text{cm}^{-1}$  for the succinic esterified samples (EPC and EBF) are attributed to the stretching vibration of the carbonyl group ( $-\text{C}=\text{O}$ ) from the succinic acid esters and the sodium carboxylate (Sehaqui et al., 2017).

The micro-morphologies of PC and BF before and after the bleaching are displayed in Fig. 1(c-f). There were obvious differences on PC and BF. The former exhibited a porous honeycomb-like structure while the latter appeared a needle-shaped structure with a large length-to-width ratio, as seen in Fig. 1(c and d). The porous PCs began to partially collapse and some BFs failed to further separate into individual fibrils after bleaching probably due to the removal of the major chemical components in cell walls in Fig. 1(e and f) (Wang et al., 2016).

Table 1 lists the chemical composition, degree of polymerization, and crystallinity of PC and BF before and after bleaching treatment. The contents of cellulose, hemicellulose, and lignin in BF were 55.4 %, 13.0 %, and 29.9 %, respectively, which was higher cellulose content but lower hemicellulose and lignin contents compared to the corresponding components (42.9 %, 17.1 %, and 32.6 %) of PC. Moreover, the cellulose contents of BBF and BPC were further increased to 89.6 % and 86.5 %, respectively, while lignin was almost entirely removed after bleaching. The average DP and crystallinity of cellulose in BF corresponding to 1579 and 69.6 % were higher than those in PC (1251 and 64.4 %) (Fig. S1). This implied that PC was a better candidate for preparation of

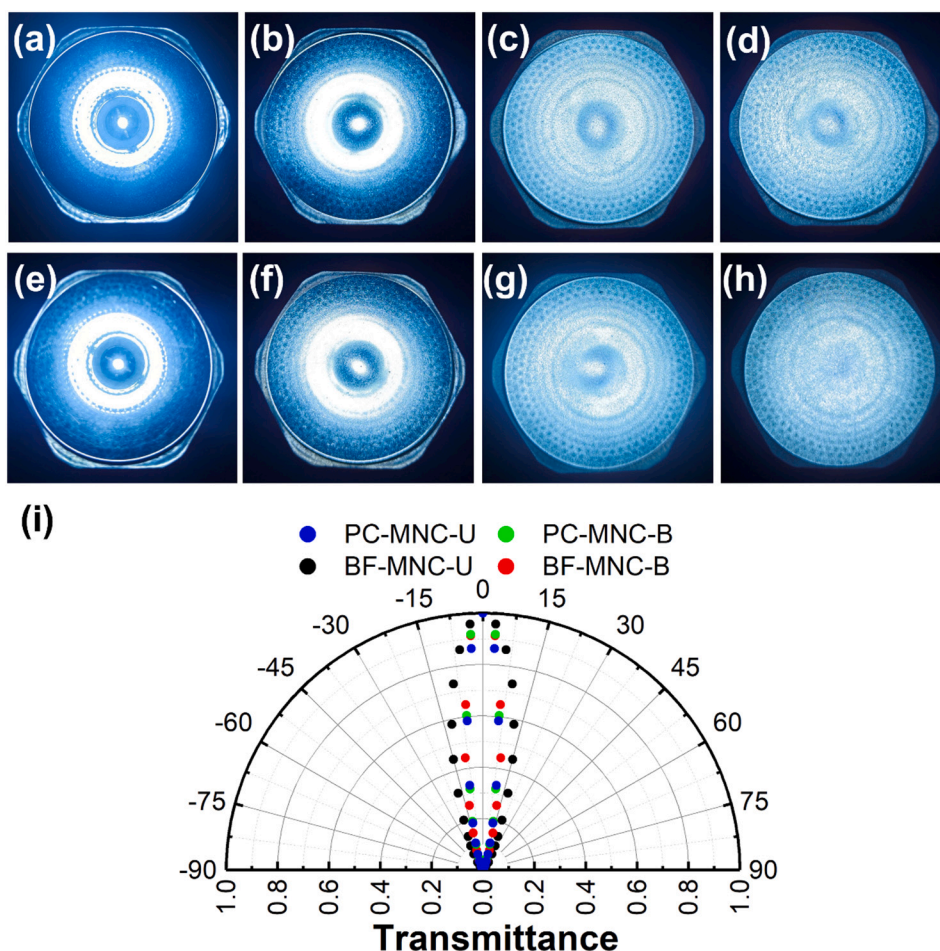


**Fig. 6.** Photographs of LED light sources without films (a) and the anti-glare effects of different films: (b) PC-MNC-M, (c) PC-MNC-B, (d) PC-MNC-U, (e) control PE film; (f) BF-MNC-M; (g) BF-MNC-B; (h) BF-MNC-U; (i) Angular distribution of intensity (wavelength = 550 nm) transmitted through films.

**Table 3**

Comparison with cellulose-based optical management films.

Sources	Methods	Transmittance (%)	Haze (%)	References
Bleached softwood kraft pulp	TEMPO-oxidized microfibrils deposited on TEMPO-oxidized cellulose nanofibrils	83.0–88.0	3.8–62.3	Yang et al., 2018
Tunicate cellulose	Mixing microfibrillated cellulose and cellulose nanofibrils	85.0	68.3	Jiang et al., 2023
Bleached hardwood kraft pulp	TEMPO-oxidized cellulose nanofiber with high-speed blending and ultrasonic homogenization	82.7	97.4	Guan et al., 2022
Bleached softwood pulp	TEMPO-oxidized wood fibers by ion exchange	90.0	93.5	Hou, Li, et al., 2022
Bleached softwood kraft pulp	Phosphorylated cellulose fibers with high-speed blending	91.0–95.0	9.0–91.0	Hou, Zhao, et al., 2022
Poplar pulp LCNF/glycerol film	TEMPO-mediated oxidation and high pressure homogenization	87.0	92.0	Zhang, Zhang, et al., 2023
Bamboo-based MNC film	Esterification of succinic anhydride with ultrasonication, high-speed blending or microfluidization	81.3–89.5	32.0–96.7	This study

micro and nano cellulose than BF in bamboo.

### 3.2. Analyses of physical, chemical, and mechanical properties of MNC

Table 2 exhibits the physical-chemical properties of MNC. It can be seen that negatively-charged carboxyl groups were successfully introduced onto the surface of cellulose by rapid succinic esterification. The average carboxyl contents (1.80–1.89 mmol/g) of MNC derived from PC were higher than those (1.69–1.76 mmol/g) derived from BF, indicating that BPC was more easily reacted with succinic anhydride than BBF. The MNC samples derived from BPC and BBF with different degrees of

nanofibrillation were obtained by ultrasonication, high-speed blending, and microfluidization. The proportions of nano-scale cellulose prepared by microfluidization were the highest among three mechanical defibrillation methods, corresponding to 96.5 % for PC-MNC-M and 93.9 % for BF-MNC-M, respectively. However, the proportion of nano-scale cellulose obtained by ultrasonication were only 28.9 % for PC-MNC-U and 20.3 % for BF-MNC-U, respectively. It was noticed that the degree of nanofibrillation for PC-derived MNC was higher than BF-derived MNC. This may be due to the fact that PC with thinner cell walls, larger cavities, and more negatively charged carboxyl groups was easily mechanically defibrillated.



Fig. 7. Mechanism of various mechanical defibrillation and their effects on the optical properties of MNC films.

In addition, compared with BPC and BBF, there was a significant decrease for the crystallinity of MNC particles from 64.4 to 42.5–53.3 % possibly due to the destruction caused by the shearing force of mechanical instruments as well as the frictional force among these various scale cellulose particles.

The micro-morphologies of micro-scale and nano-scale cellulose after centrifuging separation from the MNC suspensions are displayed in Fig. 2. Generally, the cellulose with two types of different shapes can be observed. The micro-scale cellulose components derived from PC defibrillated by ultrasonication, high-speed blending, and microfluidization appeared the thin-walled granular or bulk morphologies with the average diameters of 37.70  $\mu\text{m}$ , 35.91  $\mu\text{m}$ , and 16.25  $\mu\text{m}$ , respectively, as shown in optical and polarized optical micrographs (Fig. 2a-c), while those derived from BF displayed the slender and nodular fibril morphologies with various individual lengths corresponding to small average diameters (14.97  $\mu\text{m}$ , 12.80  $\mu\text{m}$ , and 8.46  $\mu\text{m}$ , respectively), as seen in Fig. 2(d-f). This implied that BF is the major source to isolate the cellulose microfibril.

The atomic force microscopy (AFM) images verified all nano-scale celluloses exhibited the flexible nanofibril morphologies with the longer length and the thinner width as well as varying degrees of entanglement compared to the micro-scale cellulose. The average diameters of PC-based nanocellulose after ultrasonication, high-speed blending, and microfluidization were 2.13 nm, 2.11 nm, and 1.73 nm, respectively, while those of BF-based nanocellulose were 2.26 nm, 2.08 nm, and 1.80 nm, respectively. This indicated that microfluidization had a strong defibrillation probably due to the strong shear and impact forces generated in tiny channels under the high pressure (Balasubramaniam et al., 2015). However, the relatively weak defibrillation may be achieved by the severe collisions inside PC and BF through the resultant cavities by formation and explosion of bubbles (Wang et al., 2016). The largest average aspect ratios of nanocellulose were obtained by microfluidization, corresponding to 700 and 630 for PC-MNC-M and BF-MNC-M, respectively. Therefore, PC was easier to be defibrillated than BF under the same processing conditions and produced smaller size cellulose.

Fig. 3(a-d) illustrates the thermogravimetry (TG) and differential thermogravimetry (DTG) curves of PC and BF before and after bleaching and the resultant MNC. A slight weight loss observed in 60–100  $^{\circ}\text{C}$  can be associated with the residual water and adsorbed moisture during

storage. The major weight loss occurred in 250–400  $^{\circ}\text{C}$  was related with thermal decomposition of cellulose, hemicellulose, and partial lignin (Xu et al., 2020). The onset degradation temperature ( $T_{\text{onset}}$ ) and maximum temperature ( $T_{\text{max}}$ ) for BF listed in Table S1 were higher than those of PC, indicating that the thermal stability of BF was better than PC. After purification, the thermal stabilities of BPC and BBF were similar.  $T_{\text{onset}}$  and  $T_{\text{max}}$  of MNC ranged from 302 to 310  $^{\circ}\text{C}$  and 342–348  $^{\circ}\text{C}$ . The lower thermal stability of MNC compared with the raw materials was attributed to the introduction of carboxylate groups, while mechanical disintegration had little effect (Liu et al., 2010). The MNC produced through succinic esterification pretreatment showed greater thermal stability than cellulose nanofibers produced by TEMPO oxidation ( $T_{\text{onset}} = 200$   $^{\circ}\text{C}$  and  $T_{\text{max}} = 250$   $^{\circ}\text{C}$ ) (Fukuzumi et al., 2009).

The mechanical properties of MNC films are shown in Fig. 3(e and f). The MNC films obtained by microfluidization showed the highest tensile strength and Young's modulus but the lowest elongation at break compared with the samples prepared by ultrasonication and high-speed blending. The tensile strengths and Young's modulus of PC-MNC-M films were 164.3 MPa and 8.7 GPa, respectively. As for BF-MNC-M films, they were 143.4 MPa and 8.2 GPa, respectively. This indicated that PC-based MNC had a superior tensile strength and modulus than BF-based MNC. The tensile strength of the succinic esterification MNM film ranged from 71.5 MPa to 164.3 MPa, which had a better performance for a phosphorylated cellulose light-management film ranged from 71 MPa to 152 MPa (Hou, Zhao, et al., 2022). A higher degree of nanofibrillation improved the tensile properties of film. As expected, multiscale MNC films with the highest content of micro-scale cellulose showed the weakest mechanical properties, whereas those containing the highest content of nano-scale cellulose appeared the best mechanical properties. This was because nanofibers were more aligned, enhancing the bonding between the microfibrils or microparticles and consequently promoting the strength of the films by densifying the fiber bonds.

### 3.3. Optical properties of MNC films

The digital photographs of MNC films attached to a baseboard with a logo and lifted 0.5 cm above the baseboard are shown in Fig. 4.

It can be observed that the “International Centre for Bamboo and Rattan” logos were visible beneath all films that were closely adhered to the baseboard in Fig. 4(a, b, c, g, h, and i), indicating their available

transparency. However, when the films were raised and stayed above the baseboard, the logos were obscure at varying degrees, as seen in Fig. 4(d, e, f, j, k, and l). The specific transmittance and haze values are listed in Table S2. The PC-MNC-M and BF-MNC-M films prepared by microfluidization showed the excellent transparency with the highest transmittance values of 89.5 % but the lowest haze values of 32.0 % and 41.3 %, respectively. The PC-MNC-U and BF-MNC-U films obtained by ultrasonication displayed the poor transparency with the lowest transmittance values of 84.8 % and 81.3 % but the highest haze values of 88.4 % and 96.7 %, respectively. The two parameters for PC-MNC-B and BF-MNC-B films were at the medium level.

The optical properties of the films were closely related to their microstructure, which was mainly determined by the weight ratios of micro-scale and nano-scale cellulose particles. The SEM images of the microstructure of the film on the surface and fractured surface are presented in Fig. 5. The surface and cross-sectional micro-morphologies in Fig. 5(c, f and i, l) show that there was only a small amount of micro-scale cellulose in the MNC film prepared by microfluidization. Thus, they formed a smooth surface with a homogeneous and dense microstructure inside. Most of the incident light's intensity was transmitted in the same direction, and only a small fraction was scattered, resulting in high transparency and low haze. The contents of micro-scale cellulose in the MNC films increased through ultrasonication and high-speed blending. The fibril-like microfibers were clearly seen, and the film surface was relatively rough in Fig. 5(a, b, g, and h). The existence of a light-scattering micro-scale cellulose caused the majority of light to deviate from its original path, which resulted in a high haze in the resultant films. Nano-scale cellulose filled the pores, and most incident light propagated through the film, retaining a high transmittance (Yao et al., 2016).

The anti-glare effect of MNC films on LED sources is shown in Fig. 6. The transmission light without and with the control film was obvious, which indicated that the control film did not scatter light, as seen in Fig. 6(a and e). The PC-MNC-M and BF-MNC-M films prepared by microfluidization in Fig. 6(b and f) showed low degrees of haze due to the low content of micro-scale cellulose and therefore showed only a minor anti-glare effect. After being covered by the light-scattering film prepared by high-speed blending and ultrasonication, the LED columnar light became increasingly even and gentler. When covered by the PC-MNC-U and BF-MNC-U films in Fig. 6(d and h), the LED exhibited the best anti-glare effect (Jacucci et al., 2021).

The angular distribution diagram and data of the light intensity through the highly transparent-hazy MNC films is shown in Fig. 6i and Table S3. The light transmitted intensities decrease with the increase of deflection angles for all the films. The BF-MNC-U film, with the highest proportion of micro-scale cellulose (79.7 %), produced the highest haze (96.7 %) and rendered the widest transmission angle distribution. Specifically, the light transmitted intensity of the BF-MNC-U film still maintained at 44.49 % compared with the PC-MNC-U at 10.85% and BF-MNC-B at 14.88 % when the angle was set at 15°. This implied that bamboo fibers are superior to parenchyma cells for preparing the light transmission films. A higher volume of fine nano-scale cellulose led to a denser microstructure, reducing light scattering and haze but enhancing film transparency. Moreover, the ultrasonication was more appropriate than blending as well. According to Raleigh scattering theory, the scattering cross-section is proportional to the diameter of a fiber (Song et al., 2013; Sun et al., 2018). Therefore, a higher proportion of nano-scale cellulose in the MNC films produced a higher haze and light scattering, but the transparency was slightly compromised. In addition, the PC-derived MNC film had a relatively smooth surface and a more compact fracture surface, while the BF-MNC films had a lamellar structure with gaps, resulting in a high haze.

Table 3 compares the transmittance and haze values of cellulose-based optical management films derived from various biomass resources and obtained by different physical, chemical and mechanical methods. It is seen that the tunicate cellulose-based films prepared by

mixing microfibrillated cellulose and cellulose nanofibrils displayed the transmittance of 85.0 % and haze of 65.3 %. The bleached softwood kraft pulp films obtained by depositing TEMPO-oxidized microfibers on TEMPO-oxidized cellulose nanofibrils showed relatively low transmittance (83.0–88.0 %) and haze (3.8–62.3 %). The haze of the bleached softwood kraft pulp treated by ion exchange as well as high-speed blending of phosphorylated cellulose fibers can be greatly improved to 93.5 % and 91.0 %, respectively. As for bleached hardwood kraft pulp, the mixing cellulose microfiber and TEMPO-mediated cellulose nanofiber exhibited the highest haze (97.4 %) but low haze (82.7 %). The poplar pulp LCNF/glycerol film prepared by TEMPO-mediated oxidation and high pressure homogenization exhibited the medium transmittance (87.0 %) and haze (92.0 %) level. The current bamboo-based optical management films with more environmentally-friendly chemical reagent and more facile procedure can provide an outstanding comprehensive performance with high transmittance (89.5 %) and haze (96.7 %), which can expand and enrich the high-value added applications of bamboo resources in the future.

#### 3.4. Tunable mechanism of transparent and hazy MNC films

The mechanism of various mechanical defibrillation and their effects on the optical properties of multiple micro-scale and nano-scale cellulose films with the variations of morphology, size, and micro-nano components is shown in Fig. 7. A large number of bubbles were formed, grown, and collapsed during ultrasonic vibration. The ultrasound energy can be transferred to cellulose macromolecule chains of bamboo fibers and parenchyma cells, resulting in the breakdown of the interfibrillar hydrogen bonds and then defibrillation by continuous strong colliding each other due to cavitation (Wang et al., 2016). The samples were simultaneously subjected to strong shear force, high-frequency oscillation, cavitation, and vibration when they passed through the tiny channels in microfluidization chamber, which produced the more and the smaller-size cellulose fibers (Li et al., 2014). Some bubbles were formed during agitation, which facilitated the bamboo fibers and parenchyma cells to rapidly separated as individuals. The major force for high-speed blending was the strong collision by the fast blades rotation with a mild rotational force, which split the samples into fine fragments.

According to Raleigh's scattering theory, the scattering cross section increases linearly with the diameter of the fibril (Sun et al., 2018). The more and the finer nanofibers can fill pores and thereby formed a more compact microstructure, which inhibited the light scattering and enabled them to pierce the film along the forward direction, resulting in a narrow scattering angle and a high transparency. The increase in micro-scale cellulose content raised the surface roughness and decreased the film density, causing most of the light to deviate from its original route with a wide scattering angle and inducing a high haze. The transparency and haze could be effectively tuned by changing the mechanical defibrillation method and the weight ratio of nano-scale and micro-scale cellulose.

## 4. Conclusions

Micro-scale and nano-scale cellulose derived from the parenchyma cells (PC) and bamboo fibers (BF) of *Dendrocalamus sinicus* were separated and then subjected to succinic esterification and mechanical defibrillation by ultrasonication, high-speed blending, or microfluidization. Sustainable multiscale optical management films with tunable haze were obtained by adjusting mechanical defibrillation and changing the weight ratios of micro/nanoscale cellulose. PC-derived cellulosic materials had a higher degree of fibrillation when processed by the same treatments. The MNC prepared by different mechanical treatment had different degrees of nanofibrillation, yielding the corresponding films with different optical and mechanical properties. The PC-based micro/nano cellulose (MNC) films obtained by microfluidization

with 96.5 % nanocellulose content exhibited the highest light transmittance (89.4 %) and tensile strength (164.3 MPa) but the lowest haze (32.0 %) and anti-glare ability. The BF-based MNC films obtained by ultrasonication with the lowest nanocellulose content (20.4 %) but the highest microcellulose content (79.6 %) showed the highest haze (96.6 %), a light transmittance of 81.3 %, and the outstanding anti-glare effects. The MNC films with both high in transparency (84.8–87.5 %) and haze (81.5–88.4 %) along with good strength and flexibility can be obtained by adjusting the bamboo components and mechanical defibrillation methods. This study provides a green and facile way to fabricate sustainable optical management films.

### CRedit authorship contribution statement

**Yu Chen:** Writing – original draft, Data curation. **Yuting Zhang:** Visualization, Investigation, Data curation. **Juan Long:** Data curation. **Kaimeng Xu:** Writing – review & editing, Methodology, Funding acquisition, Conceptualization. **Tuhua Zhong:** Writing – review & editing, Project administration, Methodology, Funding acquisition, Conceptualization.

### Declaration of competing interest

The authors declare that they have no known competing financial interests or personal relationships that could have appeared to influence the work reported in this paper.

### Data availability

The authors do not have permission to share data.

### Acknowledgments

We sincerely appreciated the financial support by the Fundamental Research Funds of the International Centre for Bamboo and Rattan (ICBR) (1632022025 and 1632023017), Yunnan Province Agricultural Joint Research Key Project (202301BD070001-153), Yunnan Fundamental Research Projects (202201AT070058), National Natural Science Foundation of China (NSFC) (32460434 and 32060381), the Scientific Research Funds of Educational Committee of Yunnan Province (2023Y0700), the High Level Innovative One-Ten-Thousand Youth Talents of Yunnan Province (YNWR-QNBJ-2020-203), and “111” Project (D21027).

### Appendix A. Supplementary data

Supplementary data to this article can be found online at <https://doi.org/10.1016/j.carbpol.2024.122811>.

### References

- Abe, K., & Yano, H. (2010). Comparison of the characteristics of cellulose microfibril aggregates isolated from fiber and parenchyma cells of Moso bamboo (*Phyllostachys pubescens*). *Cellulose*, 17(2), 271–277. <https://doi.org/10.1007/s10570-009-9382-1>
- Balasubramaniam, V. M. B., Martínez-Monteaegudo, S. I., & Gupta, R. (2015). Principles and application of high pressure-based technologies in the food industry. *Annual Review of Food Science and Technology*, 6(1), 435–462. <https://doi.org/10.1146/annurev-food-022814-015539>
- Chen, Y., Xiao, Y., Long, J., Xu, K., & Zhong, T. (2024). Highly transparent-hazy multiscale films made of bamboo cellulose micro- and nanomaterials through a one-pot approach. *Industrial Crops and Products*, 216, Article 118707. <https://doi.org/10.1016/j.indcrop.2024.118707>
- Fatah, I. Y. A., Abdul Khalil, H., Hossain, M. S., Aziz, A. A., Davoudpour, Y., Dungani, R., & Bhat, A. (2014). Exploration of a chemo-mechanical technique for the isolation of nanofibrillated cellulosic fiber from oil palm empty fruit bunch as a reinforcing agent in composites materials. *Polymers*, 6(10), 2611–2624. <https://doi.org/10.3390/polym6102611>
- Fukuzumi, H., Saito, T., Iwata, T., Kumamoto, Y., & Isogai, A. (2009). Transparent and high gas barrier films of cellulose nanofibers prepared by TEMPO-mediated oxidation. *Biomacromolecules*, 10(1), 162–165. <https://doi.org/10.1021/bm801065u>
- Gao, L., Chao, L., Hou, M., Liang, J., Chen, Y., Yu, H., & Huang, W. (2019). Flexible, transparent nanocellulose paper-based perovskite solar cells. *npi Flexible Electronics*, 3(1), 4. <https://doi.org/10.1038/s41528-019-0048-2>
- Guan, Q., Yang, K., Han, Z., Yang, H., Ling, Z., Yin, C., & Yu, S. (2022). Sustainable multiscale high-haze transparent cellulose fiber film via a biomimetic approach. *ACS Materials Letters*, 4(1), 87–92. <https://doi.org/10.1021/acsmaterialslett.1c00630>
- Hou, G., Li, G., Chen, H., & Fang, Z. (2022). Rapid preparation of highly transparent paper with high built-in haze by an ion exchange approach. *Chemical Engineering Journal*, 439, Article 135776. <https://doi.org/10.1016/j.cej.2022.135776>
- Hou, G., Liu, Y., Zhang, D., Li, G., Xie, H., & Fang, Z. (2020). Approaching theoretical haze of highly transparent all-cellulose composite films. *ACS Applied Materials & Interfaces*, 12(28), 31998–32005. <https://doi.org/10.1021/acsmi.0c08586>
- Hou, G., Zhao, S., Li, Y., Fang, Z., & Isogai, A. (2022). Mechanically robust, flame-retardant phosphorylated cellulose films with tunable optical properties for light management in LEDs. *Carbohydrate Polymers*, 298, Article 120129. <https://doi.org/10.1016/j.carbpol.2022.120129>
- Hu, Y., Hu, F., Gan, M., Xie, Y., & Feng, Q. (2021). Facile one-step fabrication of all cellulose composites with unique optical performance from wood and bamboo pulp. *Carbohydrate Polymers*, 274, Article 118630. <https://doi.org/10.1016/j.carbpol.2021.118630>
- Jacucci, G., Schertel, L., Zhang, Y., Yang, H., & Vignolini, S. (2021). Light management with natural materials: From whiteness to transparency. *Advanced Materials*, 33(28), 2001215. <https://doi.org/10.1002/adma.202001215>
- Jia, C., Chen, C., Mi, R., Li, T., Dai, J., Yang, Z., Pei, Y., He, S., Bian, H., & Jang, S. (2019). Clear wood toward high-performance building materials. *ACS Nano*, 13(9), 9993–10001. <https://doi.org/10.1021/acsnano.9b00089>
- Jiang, C., Wu, M., Zhang, F., Liu, C., Sun, M., & Li, B. (2023). All-tunicate cellulose film with good light management properties for high-efficiency organic solar cells. *Nanomaterials*, 13(7), 1221. <https://doi.org/10.3390/nano13071221>
- Khawas, P., & Deka, S. C. (2016). Isolation and characterization of cellulose nanofibers from culinary banana peel using high-intensity ultrasonication combined with chemical treatment. *Carbohydrate Polymers*, 137, 608–616. <https://doi.org/10.1016/j.carbpol.2015.11.020>
- Li, J., Wang, Y., Wei, X., Wang, F., Han, D., Wang, Q., & Kong, L. (2014). Homogeneous isolation of nanocelluloses by controlling the shearing force and pressure in microenvironment. *Carbohydrate Polymers*, 113, 388–393. <https://doi.org/10.1016/j.carbpol.2014.06.085>
- Li, X., Li, J., Shen, X., Cao, M., Wang, Y., Zhang, W., Xu, Y., Ling, Z., Chen, S., & Xu, F. (2024). Transparent cellulose/lignin composite films with adjustable haze and UV-blocking performance for light management. *ACS Sustainable Chemistry & Engineering*, 12(14), 5427–5435. <https://doi.org/10.1021/acssuschemeng.3c07076>
- Liu, C. F., Zhang, A. P., Li, W. Y., Yue, F. X., & Sun, R. C. (2010). Succinylation of cellulose catalyzed with iodine in ionic liquid. *Industrial Crops and Products*, 31(2), 363–369. <https://doi.org/10.1016/j.indcrop.2009.12.002>
- Qu, R., Tang, M., Wang, Y., Li, D., & Wang, L. (2021). TEMPO-oxidized cellulose fibers from wheat straw: Effect of ultrasonic pretreatment and concentration on structure and rheological properties of suspensions. *Carbohydrate Polymers*, 255, Article 117386. <https://doi.org/10.1016/j.carbpol.2020.117386>
- Segal, L., Creely, J. J., Martin, A. E., Jr., & Conrad, C. M. (1959). An empirical method for estimating the degree of crystallinity of native cellulose using the X-ray diffractometer. *Textile Research Journal*, 29(10), 786–794. <https://doi.org/10.1177/004051755902901003>
- Sehaqui, H., Kulasinski, K., Pfenninger, N., Zimmermann, T., & Tingaut, P. (2017). Highly carboxylated cellulose nanofibers via succinic anhydride esterification of wheat fibers and facile mechanical disintegration. *Biomacromolecules*, 18, 242–248. <https://doi.org/10.1021/acs.biomac.6b01548>
- Shi, Y., Wu, M., Ge, S., Li, J., Alshammari, A. S., Luo, J., ... Chen, X. (2025). Advanced functional electromagnetic shielding materials: A review based on micro-nano structure interface control of biomass cell walls. *Nano-Micro Letters*, 17, 3. <https://doi.org/10.1007/s40820-024-01494-2>
- Sluiter, A., Hames, B., Ruiz, R., Scarlata, C., Sluiter, J., Templeton, D., & Crocker, D. (2008). Determination of structural carbohydrates and lignin in biomass. *Laboratory Analytical Procedure*, 1617(1), 1–16.
- Song, S., Sun, Y., Lin, Y., & You, B. (2013). A facile fabrication of light diffusing film with LDP/polyacrylates composites coating for anti-glare LED application. *Applied Surface Science*, 273, 652–660. <https://doi.org/10.1016/j.apsusc.2013.02.103>
- Sun, H., Liu, Y., Guo, X., Zeng, K., Mondal, A. K., Li, J., ... Chen, L. (2021). Strong, robust cellulose composite film for efficient light management in energy efficient building. *Chemical Engineering Journal*, 425, Article 131469. <https://doi.org/10.1016/j.cej.2021.131469>
- Sun, X., Wu, Q., Zhang, X., Ren, S., Lei, T., Li, W., ... Zhang, Q. (2018). Nanocellulose films with combined cellulose nanofibers and nanocrystals: Tailored thermal, optical and mechanical properties. *Cellulose*, 25(2). <https://doi.org/10.1007/s10570-017-1627-9>, 1103-1115, 1103-1115.
- Szcześniak, L., Rachocki, A., & Tritt-Goc, J. (2008). Glass transition temperature and thermal decomposition of cellulose powder. *Cellulose*, 15, 445–451. <https://doi.org/10.1007/s10570-007-9192-2>
- Wang, H., Zhang, X., Jiang, Z., Yu, Z., & Yu, Y. (2016). Isolating nanocellulose fibrils from bamboo parenchymal cells with high intensity ultrasonication. *Holzforschung*, 70(5), 401–409. <https://doi.org/10.1515/hf-2015-0114>
- Xu, K., Shi, Z., Lyu, J., Zhang, Q., Zhong, T., Du, G., & Wang, S. (2020). Effects of hydrothermal pretreatment on nano-mechanical property of switchgrass cell wall and on energy consumption of isolated lignin-coated cellulose nanofibrils by mechanical grinding. *Industrial Crops and Products*, 149, Article 112317. <https://doi.org/10.1016/j.indcrop.2020.112317>

- Yang, W., Jiao, L., Liu, W., Deng, Y., & Dai, H. (2018). Morphology control for tunable optical properties of cellulose nanofibrils films. *Cellulose*, 25, 5909–5918. <https://doi.org/10.1007/s10570-018-1974-1>
- Yao, Y., Tao, J., Zou, J., Zhang, B., Li, T., Dai, J., ... Henderson, D. (2016). Light management in plastic–paper hybrid substrate towards high-performance optoelectronics. *Energy and Environmental Science*, 9(7), 2278–2285. <https://doi.org/10.1039/c6ee01011c>
- Zhang, T., Yuan, T., Xiao, X., Peng, H., Fang, X., Wang, K., Liu, X., & Li, Y. (2022). Transparent and shape-memory cellulose paper reinforced by vitrimer polymer for efficient light management and sustainability. *Cellulose*, 29(16), 8781–8795. <https://doi.org/10.1007/s10570-022-04797-y>
- Zhang, W., Zhang, X., Ren, S., Dong, L., Ai, Y., Lei, T., & Wu, Q. (2023). Lignin containing cellulose nanofiber based nanopapers with ultrahigh optical transmittance and haze. *Cellulose*, 30(9), 5967–5985. <https://doi.org/10.1007/s10570-023-05244-2>
- Zhang, X., Guo, F., Yu, Z., Cao, M., Wang, H., Yang, R., Yu, Y., & Salmén, L. (2022). Why do bamboo parenchyma cells show higher nanofibrillation efficiency than fibers: An investigation on their hierarchical cell wall structure. *Biomacromolecules*, 23(10), 4053–4062. <https://doi.org/10.1021/acs.biomac.2c00224>
- Zhang, X., Huang, H., Qing, Y., Wang, H., & Li, X. (2020). A comparison study on the characteristics of nanofibrils isolated from fibers and parenchyma cells in bamboo. *Materials*, 13(1), 237. <https://doi.org/10.3390/ma13010237>
- Zhang, Y., Wang, S., You, S., Wang, J., Wang, J., Jia, L., Zhang, H., & Zhang, M. (2023). Fabrication of transparent and hazy cellulosic light-management film for enhancing photon utilization in photocatalytic membrane process. *Journal of Membrane Science*, 685, Article 121923. <https://doi.org/10.1016/j.memsci.2023.121923>
- Zhao, B., Vasilopoulou, M., Fakhruddin, A., Gao, F., Mohd Yusoff, A. R. B., Friend, R. H., & Di, D. (2023). Light management for perovskite light-emitting diodes. *Nature Nanotechnology*, 18(9), 981–992. <https://doi.org/10.1038/s41565-023-01482-4>
- Zhao, X., Ye, H., Chen, F., & Wang, G. (2024). Bamboo as a substitute for plastic: Research on the application performance and influencing mechanism of bamboo buttons. *Journal of Cleaner Production*, 446, Article 141297. <https://doi.org/10.1016/j.jclepro.2024.141297>
- Zhong, T., Dhandapani, R., Liang, D., Wang, J., Wolcott, M. P., Fossen, D. V., & Liu, H. (2020). Nanocellulose from recycled indigo-dyed denim fabric and its application in composite films. *Carbohydrate Polymers*, 240, Article 116283. <https://doi.org/10.1016/j.carbpol.2020.116283>
- Zhou, J., Fang, Z., Chen, K., Cui, J., Yang, D., & Qiu, X. (2022). Improving the degree of polymerization of cellulose nanofibers by largely preserving native structure of wood fibers. *Carbohydrate Polymers*, 296, Article 119919. <https://doi.org/10.1016/j.carbpol.2022.119919>
- Zhu, H., Fang, Z., Wang, Z., Dai, J., Yao, Y., Shen, F., Preston, C., Wu, W., Peng, P., & Jang, N. (2016). Extreme light management in mesoporous wood cellulose paper for optoelectronics. *ACS Nano*, 10(1), 1369–1377. <https://doi.org/10.1021/acsnano.5b06781>